

EXPERIMENTAL AND COMPUTATIONAL ANALYSIS FOR OPTIMIZATION OF SEAWATER BIODEGRADABILITY USING PHOTO CATALYSIS

NAYEEMUDDIN MOHAMMED^{1*}, PUGANESHWARY PALANIANDY¹,
FEROZ SHAIK² AND HIREN MEWADA²

¹*School of Civil Engineering, Universiti Sains Malaysia, Penang, Malaysia*
²*Prince Mohammad Bin Fahd University, Al Khobar, Kingdom of Saudi Arabia*

*Corresponding author: mnayeemuddin@student.usm.my

(Received: 11 November 2022; Accepted: 20 March 2023; Published on-line: 4 July 2023)

ABSTRACT: Seawater pollution is a significant global environmental problem. Various technologies and methods have been used to remove the contaminants found in saltwater. This experimental study investigates the degradation of contaminants present in seawater using solar photocatalysis, where a combination of TiO₂ and ZnO was used. The effects of catalyst dosage, pH, and reaction duration were assessed using percentage removal efficiencies of total organic carbon (TOC), chemical oxygen demand (COD), biological oxygen demand (BOD), and biodegradability (BOD/COD). Biodegradability is essential for removing pollutants from saltwater and plays a vital role. The higher the biodegradability, the more efficient the treatment procedure will be. The most effective percentage reduction rates from the experimental data obtained were TOC=59.80%, COD=75.20%, BOD=23.94%, and biodegradability=0.055. For modeling, optimizing, and assessing the effects of parameters, the Design Expert based on Box Behnken design (RSM-BBD) and a predictive model based on the MATLAB adaptive neuro-fuzzy inference system (ANFIS) tools were used. The coefficient of determination R² was found to be 0.977 for the RSM-BBD model and 0.99 for the ANFIS model. According to the RSM-BBD design, the maximum percentage pollutant elimination efficiencies were found to be TOC=55.4, COD=73.4, BOD=23.70%, and BOD/COD=0.054, but for the ANFIS model, they were TOC=59.4, COD=75.4, BOD=24.1%, and BOD/COD=0.055. It was discovered that the ANFIS model outperformed RSM-BBD in process optimization.

ABSTRAK: : Pencemaran air laut adalah masalah alam sekitar global yang ketara. Pelbagai teknologi dan kaedah telah digunakan bagi menyingkirkan pencemaran yang dijumpai dalam air laut. Kajian eksperimen ini menilai degradasi pencemaran yang hadir dalam air laut menggunakan fotopemangkin, di mana kombinasi TiO₂ dan ZnO digunakan. Kesan dos pemangkin, pH, dan tempoh reaksi dipantau menggunakan peratus kecekapan penyingkiran jumlah karbon organik (TOC), keperluan kimia oksigen (COD), keperluan biologi oksigen (BOD), dan kebolehdegradasian (BOD/COD). Kebolehdegradasian adalah sangat penting bagi menyingkirkan bahan cemar dari air laut dan berperanan penting. Semakin tinggi kebolehdegradasian, semakin cekap prosedur rawatan. Peratus kadar pengurangan yang paling berkesan daripada data eksperimen adalah didapati pada TOC=59.80%, COD=75.20%, BOD=23.94%, dan biodegradasi=0.055. Bagi mengkaji kesan parameter terhadap model, kadar optimum, dan memantau keberkesanan parameter, kaedah Pakar Reka Bentuk pada rekaan Kotak Behnken (RSM-BBD) dan model ramalan berdasarkan sistem pengaruh menggunakan sistem MATLAB iaitu Inferens Neural-Fuzi Boleh Suai (ANFIS) digunakan. Pekali penentu R² terhasil pada 0.977 bagi model RSM-

BBD dan 0.99 pada model ANFIS. Berdasarkan reka bentuk RSM-BBD, peratus maksimum keberkesanan penyingkiran bahan cemar dijumpai pada TOC=55.4, COD=73.4, BOD=23.70%, dan BOD/COD=0.054, tetapi bagi model ANFIS, TOC=59.4, COD=75.4, BOD=24.1%, dan BOD/COD=0.055. Model ANFIS adalah lebih berkesan daripada model RSM-BBD dalam proses pengoptimuman.

KEYWORDS: *solar photocatalysis; saltwater/seawater; titanium dioxide; zinc oxide; biodegradability; RSM-Box Behnken; ANN-Anfis*

1. INTRODUCTION

The requirement for fresh and clean water has been increasing day by day. The demand for or availability of drinkable water is a major concern due to the global population rise. Seawater is a major source of freshwater generation, but it also contains several organic, inorganic, and biological contaminants in addition to salt. Before seawater is given to the primary desalination process, these contaminants must be treated. Many traditional techniques are employed to treat the contaminants found in seawater [1], but recently, sophisticated oxidation techniques have been used to remediate the contaminants in saline water.

Natural solar light and artificial UV radiation sources were utilized in heterogeneous photocatalysis using TiO₂ as a photocatalyst. Utilizing photocatalytic reactors, organic contaminants, such as phenol and benzoic acid, were removed from seawater. A semiconductor, such as TiO₂, SnO₂, ZnO, and PbO, served as a photocatalyst in this process and was exposed to artificial and natural light [2]. Seawater contaminants can be degraded by solar photocatalysis, which has been well-defined by the process of solar photocatalysis mechanism [3,4].

Numerous studies have used the solar photocatalytic degradation mechanism to remove contaminants found in saltwater. A batch recirculation reactor system was used to study the photo degradation of contaminants found in saltwater. By assessing different parameters such as TOC, total dissolved solids (TDS), COD, and total inorganic carbon, the performance of photocatalytic degradation was assessed combining TiO₂ photo catalyst and polyamide. The solar photo degradation phase saw a significant parameter drop [5]. Using a Yb-TiO₂-rGO photo catalyst, phenol in saline water was significantly reduced throughout the sun photocatalytic degradation process. To prevent salt ions from adhering to the photocatalyst, ethylene glycol was grafted onto the catalyst [6]. A photocatalyst (TiO₂) that had been immobilized in plug flow reactors was used with an artificial light source (UV lamp) to investigate the breakdown of the model of organic molecule benzoic acid to gauge the photocatalytic performance. Significant benzoic acid decomposition was seen using plug flow reactors of various diameters. Under various circumstances, photocatalysis has been used and shown to be a viable technique for purifying phenolic wastewater. In a batch reactor with a recycle stream, photocatalysis was used to completely mineralize the phenol [7]. Researchers looked at the efficiency of photocatalytic degradation of diesel impurities present in saltwater by studying the sun photocatalytic destruction of those pollutants. The initial concentration of diesel contaminants, pH, catalyst ratio, and dosage were changed. The visible photocatalytic degradation mechanism resulted in a 78.7% degradation of diesel pollutants [8]. The water produced by the oil industry, which contained both organic and inorganic contaminants, underwent nano-solar photocatalysis. Using a TiO₂ catalyst and free

solar energy, experiments were carried out in batch and continuous reactors. It was found that the amount of contaminants in oil-produced water had significantly decreased [9].

A thorough overview of numerous photocatalytic research using saltwater and saline industrial effluent, including oil-generated water, was presented by Nayeem et al. [10]. Photocatalysis refers to the acceleration of a photochemical reaction in the presence of a catalyst. The photocatalytic efficiency in photo-generated catalysis depends on the catalyst's ability to generate electron-hole pairs and free radicals capable of secondary reactions. Furthermore, it is employed in numerous processes known as the Advanced Oxidation Process (AOP) [11]. The photocatalytic reaction breaks down the harmful molecules without leaving any residue, obviating the need to transport sludge to a landfill. An additional advantage is that the catalyst has a long lifespan, and there is no requirement for chemicals in the process, keeping the operation simple and financially viable [12]. An oxidant that absorbs UV light and reacts with water to generate highly reactive OH radicals could be introduced during UV irradiation to optimize elimination efficiency. The most common oxidants are hydrogen peroxide (H_2O_2) and ozone. During the experiments, it was revealed that the absorbance accuracy of H_2O_2 is dependent on its concentration. Therefore, the efficiency of the water treatment system increases with H_2O_2 concentration [13].

For low boron concentrations in genuine desalinated seawater, UiO-66-NH₂/GO/Fe₃O₄ shows good adsorption uptake (22.46 mg/g). A novel technique of magnetic composite with a metal-organic frame was employed in the desalination of salt water to remove boron. The single-factor design model was carried out to study the ideal parameter settings using the response surface approach and the MATLAB program ANN tool. The maximal temperature, 318 K, pH 3.38, and dose of 99.1 mg/L were discovered. Both approaches have demonstrated a good ability to anticipate the adsorption process [14] accurately. For the statistical analysis, Hashemi et al. [15] used pipette-tip solid phase extraction with molecularly imprinted polymer and an RSM-BBD model with seven variables at three levels to determine the presence of methyl red in seawater. The computed average recoveries ranged from 84.0 to 98.0 percent, with a mean of 2.5 - 6.7 percent. For the breakdown of tetracycline, a TiO₂ photo catalyst in powdered form was used to treat contaminants found in seawater. Due to the strong visible light reaction, it is observed that after 20 hours, the removal of tetracycline from seawater by PU sponge-filled spheres had achieved 80%, offering the greatest performance [16]. The necessary studies to investigate the impacts of yeast extract, whey, heating temperature, and Caspian Sea water were designed using a central composite design.

According to the response surface method, the maximal specific urease activity (16.50 mm urea.min⁻¹. OD⁻¹) could be attained with 9.94 gL⁻¹ of yeast extract, 23.43 gL⁻¹ of whey, 128.6 °C of heating, and no seawater [17]. The ANN has the advantage of not requiring the central composite design before experimentation and being a continuously improving prediction approach as more data becomes available. Still, the RSM has a modest advantage in model accuracy [18]. A three-factor and three-level Box Behnken design was used to investigate the novel core-shell micro-structured nanocomposites with inner seawater for syngas/air fire prevention. Two mathematical models were created to examine the interactions between the parameters for salt rejection and to permeate flow in RO membranes [19]. Ions in seawater physically and chemically interact with mineral species, making the flotation and thickening processes harder to operate. ANOVA and RSM-based modeling are used to identify the variables that affect the variable of interest, which is then

optimized. The design of experiments (DOE) establishes the number of experiments needed and the values of the independent and dependent variables [20]. During training, the developed ANN model demonstrated a good agreement between prediction and experimental data, with good statistical metrics values (RMSE, MAE, and AARD). According to ANN, permeate conductivity, flow rate, and recovery were predicted with coefficients of determination of 0.969, 0.942, and 0.963, respectively [21].

The optimization of experimental variables to ascertain the impact of independent factors on the responses has frequently used response surface methods. The Box Behnken tool was used to reduce the number of experiments in RSM with the best response. The pH concentration was found to have the best COD elimination percentage [22, 23]. The establishment of a linear or nonlinear relationship between water salinity and its controlling factors (such as water table, evaporation, and distance to saltwater bodies) and the use of those relationships for the prediction of water salinity for regions with low data points have shown the capacity of ML models to model groundwater salinity [24]. The independent variables considered in ANN were pH, POME concentration, pressure, time, and one hidden layer and output layer. It was noted that in the filtration process, the ANN accurately displays the projected optimum values near the experimental data [25,26]. Response surface approach and a genetic algorithm tool were used to undertake statistical modeling in order to obtain the desirability function and forecast values. It was found that the RSM-GA predicted the experimental values accurately [27,28]. Utilizing RSM (Design Expert) and ANN-LM, a statistical model with three independent variables was created. The removal elimination of COD, TOC, BOD, and biodegradability were predicted by this model [29].

Numerous studies have used the MATLAB tool to predict response variables using ANN, ANFIS, FIS, and other models. A fuzzy system is the first stage in building a network of fuzzy systems and can be created by "if-then" rules. The mathematical techniques are known as the recurrent network (RN), time-lagged recurrent network (TLRN), ANN, and ANFIS are directly derived from the workings of the human brain [30]. These methods are promising for simulating response variables and can also be used with nonlinear systems due to their simplicity. When the relationship between the input and output variables is unknown, and it is impossible to identify the system by mathematical problem, the robust application known as the fuzzy inference system was utilized [31].

Utilizing RSM-BBM and ANN-ANFIS, a few studies have been published on optimizing the removal of contaminants from saltwater using solar photocatalytic degradation. To find the ideal values, polynomial quadratic models were constructed. It was discovered that the central composite design was a reliable and accurate forecast. With five input variables, a Genetic Algorithm was used as a tool in ANN and RSM [32]. The term "biodegradability" refers to the BOD/COD ratio. The elimination process of contaminants from seawater depends on biodegradability and a higher biodegradability can increase the effectiveness of the treatment approach. In addition, there will be a significant decrease in fouling characteristics during the seawater treatment process due to the high biodegradability. However, no research has reported the natural sunlight-based biodegradability of saltwater combining photocatalysts with RSM-BBD and ANFIS applications. The proposed approach uses the combination of TiO₂ and ZnO photocatalysis processes to examine the biodegradability of saline water. The process was validated using RSM-BBD and ANFIS to assess the model and optimize and investigate the relationship between the parameters.

2. MATERIALS AND METHODS

A 5 L sample of salt water was taken at a depth of 10 m from the water's surface, 2.3 km from Khobar Beach in the Kingdom of Saudi Arabia. Commercial TiO₂ Degussa P-25 (80% A-20% R) from Evonik Industries in Germany, which is 99.9% pure, and ZnO (99.9 percent pure, APS:20 nm) from mkNano in Canada were used as the catalysts total carbon analyzer (Shimadzu), thermal scientific Orion COD 125, and AQ 400 were used to measure COD and TOC, respectively. Thermo Fisher Scientific's BOD incubator with a complete water analysis kit (Eutech PCD 650) was used to measure the DO and BOD estimation, and a pH meter (JENWAY 3520) was used to measure the pH value. Table 1 displays the initial properties of seawater.

2.1 Experimental Procedure

Figure 1 depicts an experimental setup sketch for the batch investigations. As a batch reactor, a 1500 mL glass beaker with a magnetic stirrer was utilized. A 1000 mL sample of seawater was obtained in a batch reactor setup, and catalysts TiO₂ and ZnO were added. Between 10:00 AM to 2:00 PM, the photocatalytic reaction was carried out in the open air while stirring with a magnetic stirrer. At regular intervals, the samples were brought out for examination. The measured parameters were calculated by percentage removal efficiencies using equation 1.

$$\text{Percentage removal} = \frac{(P_o - P_f)}{P_o} \times 100 \quad (1)$$

where, P₀ and P_f are the starting and final concentrations in mg/L.

Table 1: Initial parameters for a seawater sample

Parameter	Values
TOC (mg/L)	2.74
COD (mg/L)	111
BOD (mg/L)	1.75
pH	8.665
Biodegradability, BOD/COD	0.0157

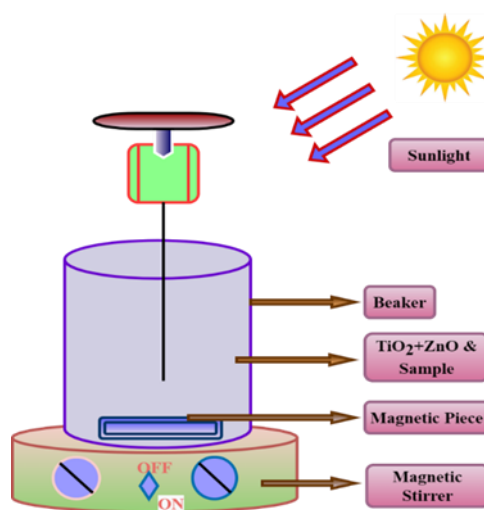


Fig. 1: The batch reactor's experimental setup.

2.2 Statistical Analysis Theoretical Model Description

2.2.1 RSM-Box Behnken Statistical Modelling

Design Expert response surface methodology is one of the major strategies for detecting and illustrating the cause-and-effect relationship between genuine average responses and input control variables influencing responses. For the statistical experimental designs, modelling approaches, regression modelling, prediction, and optimization, the Design-Expert version-11.1-2.0, State-Ease Inc. MN, USA-based Box Behnken Design of response surface methodology was used. RSM combines mathematical methods with statistical analysis to fit the second-order or quadratic model. The Box Behnken Design only needs three levels of each component, such as lower, mid, and upper level, with randomized type, in contrast to the central composite design, which needs five levels of factors. BBD offers greater refining, optimization, and precision than CCD because it is almost rotatable and requires fewer experimental runs. After essential factors are found during the screening of factorial trials, it is also utilized to investigate the effects of quadratic factors. The phases in the RSM-BBD method's strategy are shown in Fig. 2. In the RSM explained by equation 2, the Box Behnken Design utilized the generalized model equation for the second-order polynomial [33].

$$Y = (A_0) + \sum (A_i x_i) + \sum (A_{ii} x_i^2) + \sum (A_{ij} x_i x_j) \quad (2)$$

The input variables (i) and (j) are coded values in this case. The parameter or quadratic value is X_i^2 . The linear, interaction terms, intercept, linear regression, and quadratic coefficients for intercept are A_0 , A_i , A_{ij} , and A_{jj} . Y stands for the output variables, which include percentages of TOC, COD, BOD, and biodegradability removal efficiencies. To ascertain variable interaction, the statistical significance of models, and the impacts of research variables, ANOVA (analysis of variance) was performed. The equations in the quadratic-polynomial model were determined by the coefficient of determination (R^2), and the significance of regression coefficients using the F-test was evaluated at probabilities (P) 0.001 and 0.01. The 3-dimensional surface plots represent the maximum or ideal extraction conditions. An additional confirmation experiment was conducted to verify the statistical experimental procedures [34].

2.2.2 ANN-ANFIS Statistical Modelling

In this approach, an adaptive neuro-fuzzy inference system was created using MATLAB programming to discover the best parameters for the percentage removal elimination of input and output pairs (ANFIS). The ANFIS is a standard mathematical tool based on artificial intelligence and is used to model complicated nonlinear problems utilizing artificial neural network learning and neuro-fuzzy interference techniques based on the Sugeno first-order system [35]. The system's behavior can be analyzed with large datasets. Therefore, there is a need for system modeling to estimate the output for unseen datasets which fall within range or outside range. ANFIS is one of the powerful tools for such nonlinear time series analysis. This work uses ANFIS modeling to obtain a nonlinear input and output mapping.

Additionally, it employed a hybrid learning algorithm that included the least squares and backpropagation learning algorithm approaches. Figure 3 shows the first-order Sugeno-type inference system's complete ANFIS architecture was built using three

inputs, four outputs, and five layers. The models were constructed using 70% training, 30% testing, and 40% model validation [36].

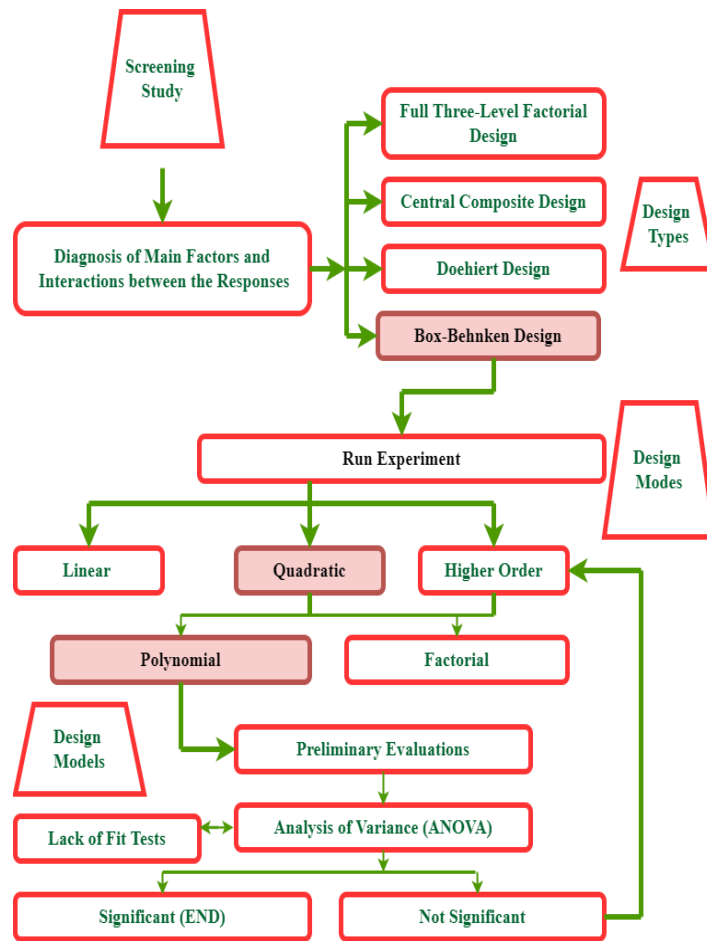


Fig. 2: Procedure for RSM - Box-Behnken [34].

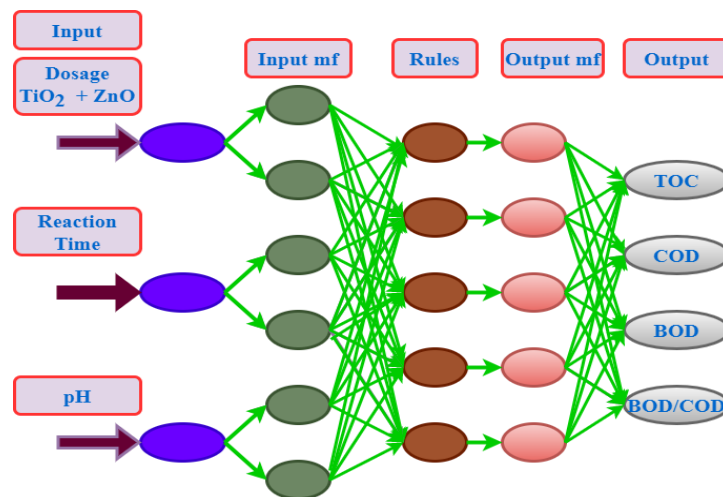


Fig. 3: Schematic diagram of Architectural Network of ANFIS model [36].

Model correctness was measured using several error estimates, such as RMSE and R^2 . This ANFIS m was created using the first-order Sugeno model with fuzzy IF-THEN techniques. The roles of each of the five layers were described in terms of two rules (equations 3 and 4) in the section that follows rules 1 and 2 [37].

$$\text{Rule 1: If } (x) \text{ is } (A_1) \text{ and } (y) \text{ is } (B_1), \text{ then } (f_1) = p_1(x) + q_1(y) + (r_1) \quad (3)$$

$$\text{Rule 2: If } (x) \text{ is } (A_2) \text{ and } (y) \text{ is } (B_2), \text{ then } (f_2) = p_2(x) + q_2(y) + (r_2) \quad (4)$$

where $p_1, p_2, q_1, q_2, r_1,$ and r_2 are the output coefficient functions that will be computed during testing, training, and validation and where x' and y' are the inputs and $A_1, A_2, B_1,$ and B_2 are the fuzzy sets.

The input variables are passed from layer 1 to layer 2, also called the independent layer or input layer. Node I has an adaptive node output expressed by Eq. 5 and Eq. 6.

$$O_i = \mu_{ai}(x), \quad \text{for } (i) = 1, 2 \quad (5)$$

$$O_i = \mu_{bi-2}(y), \quad \text{for } (i) = 3, 4 \quad (6)$$

Rule nodes are the second tier. Each input's independent values are multiplied by one another and are designated by a circle with the label "fixed nodes, non-adaptive", where w_i is given as weights and is as follows by Eq. 7:

$$O_i^2 = (w_i) = (\mu_{ai})(x) (\mu_{bi})(y) \quad \text{for } (i) = 1, 2 \quad (7)$$

The third layer with the letter N, is referred to as the layer of average nodes or the normalization layer by Eq. 8.

$$O_i^3 = (w_i) = (w_i)/(w_1 + w_2) \quad \text{for } (i) = 1, 2 \quad (8)$$

Layer 4 is where defuzzification occurs; it is also referred to as the layer of subsequent nodes because, in this layer, the output layer is coupled with the preceding layer using the Sugeno fuzzy function by Eq. 9.

$$O_i^4 = w_i (f_i) = w_i [p_i(x) + q_i(y) + r_i] \quad \text{for } i = 1, 2 \quad (9)$$

The output layer is the fifth and final layer. It is denoted by the node with the name " Σ ," which ultimately determines total output and does so by equation 10.

$$O_i^5 = f_{out} = \sum w_i (f_i) \quad (10)$$

The final output Eq. 11 can be written as:

$$f_{out} = w_1(x) p_1 + w_1(y) (q_1) + w_1(r_1) + w_2(x) (p_2) + w_2(y) (q_2) + w_2(r_2) \quad (11)$$

It can be seen from the aforementioned Eq. 3 to Eq. 11 that the ANFIS model depends on the performance of specific parameters, such as the center, and must be appropriately calibrated.

The design model contains 27 datasets with measured values of dosage, time, and pH. The ANFIS modeling has two phases: training and testing. Therefore, the dataset was divided into training and testing sets. The division of the dataset was obtained with random permutation, and the model was repeated multiple times to get the best modeling. Fuzzy C-mean clustering with Sugeno-rule is used in the ANFIS modeling. Three individual models were developed to estimate three properties, i.e., TOC, COD, and BOD. The modeling needs an appropriate selection of various parameters, including the number of memberships,

clusters, iterations, and epochs. The optimum parameters are obtained by repeating the experiment and analyzing the error obtained in predicted values. For choosing the optimum model, Mean Square Error (MSE), Root Square Error (RMSE), and Correlation Coefficient (R^2) were utilized as performance parameters. A lower value of MSE, RMSE, and a higher value of R^2 indicates superior system modeling. Let $Xp(i)$ is the predicted value from ANFIS modeling and $Xt(i)$ is the actual experimental response. If the total data is N , then quantitative parameters can be calculated using the Eqs. 12-14. The independent or input layer in this statistical modeling of the ANFIS technique comprises three neurons, and the output layer has one [38]. The three ANFIS models will be created and examined for four output responses in this investigation, including TOC, COD, BOD, and BOD/COD, respectively. All of the model's statistical parameters were compared, and the following equations below [39] can be used to assess the trained network's ultimate performance:

$$\text{Root mean square error (RMSE)} = \sqrt{\frac{1}{N} \sum_{i'=1}^N [Xp, i' - Xt, i]^2} \quad (12)$$

$$\text{Mean square error (MSE)} = \frac{1}{N} \sum_{i'=1}^N [(Xp, i' - Xt, i')]^2 \quad (13)$$

$$\text{Standard error (SE)} = S = \sqrt{\frac{1}{N-1} \sum_{i=1}^N [(Xp - \widehat{Xt})]^2} \quad (14)$$

3. RESULTS AND DISCUSSION

Equation 1 was employed to calculate the experimental data's percentage elimination efficiencies and biodegradability.

3.1 Effect of Combined Catalyst TiO_2 and ZnO Dosage

Figure 4 shows the combined TiO_2 and ZnO photocatalyst dose variation for the percentage elimination efficiency of reactions like TOC, COD, and BOD, and biodegradability. The reactants were charged into the batch reactor, thoroughly mixed, and the photocatalyst concentration was gradually increased to 4 g/L maximum. Every hour, samples were collected, and the parameters were examined.

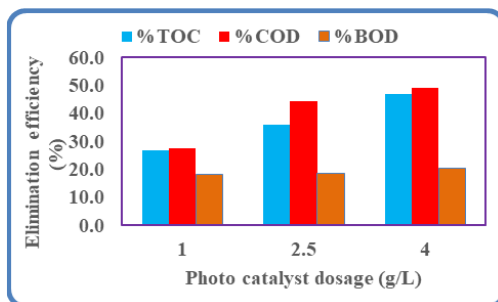


Fig. 4: Percent (%) elimination efficiency versus photocatalyst dosage.

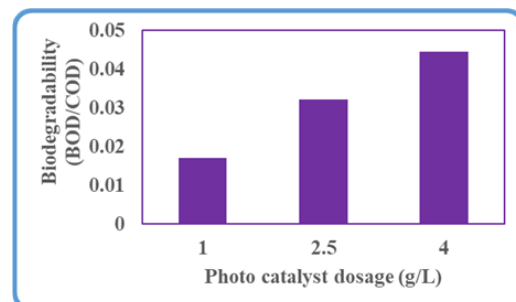


Fig. 5: Biodegradability (BOD/COD) versus photocatalyst dosage.

The parameter's percentage increases were analyzed, and the final data was plotted [3]. It was discovered that there was a significant increase in TOC, COD, and BOD up to 4 g/L of dosage of combination photocatalyst due to an increase in photonic energy availability from 10:00 AM to 2 PM. Furthermore, it was discovered that the degradation of pollutants

appears on the greater side at higher dosages of combination catalysts, which could be attributed to the availability of more active sites on the catalyst [1]. The highest percentage removal efficiency was reported to be 46.98, 49.3, and 20.23 percent for TOC, COD, and BOD at a dosage of 4 g/L, a reaction time of 300 min, and a pH of 9. Nevertheless, as shown in Fig. 5, biodegradability was found to be 0.045.

3.2 Effect of Reaction Time

Figure 6 shows the output variable's percentage removal efficiencies, depicted with reaction times. The reaction time steadily grew from 0 to 180 minutes before rapidly decreasing to 300 minutes [13]. TOC and COD increase sharply up to 180 min and decrease at 300 min [2]. The highest percentage efficiency for TOC, COD, and BOD were determined to be 60, 75.2 and 24% respectively, for reaction times of 180 minutes, dosages of 4 g/L and pH values of 9 and 0.05 for biodegradability Fig. 7.

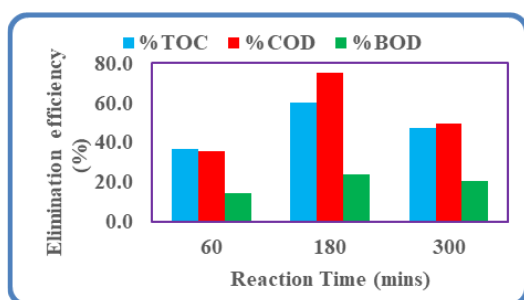


Fig. 6: Percent (%)% elimination efficiency versus reaction time.

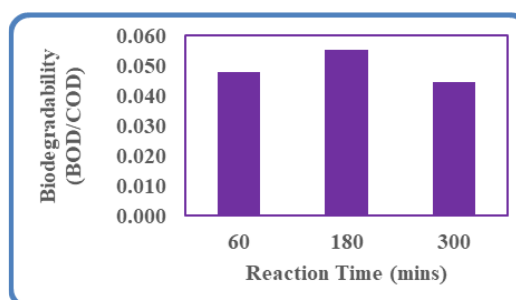


Fig. 7: Biodegradability (BOD/COD) versus reaction time.

3.3 Effect of Percentage Removal Efficiency versus pH

Figure 8 displays the output response's percentage elimination efficiencies concerning pH value at various variations [4]. It was reported that the maximum removal efficiencies were found to be TOC = 47, COD = 49.2, and BOD = 20.23 %, respectively [13]. Whereas biodegradability = 0.045 at pH = 9, reaction time = 300 minutes and dosage of combined catalyst = 4 g/L as shown in Fig. 9.

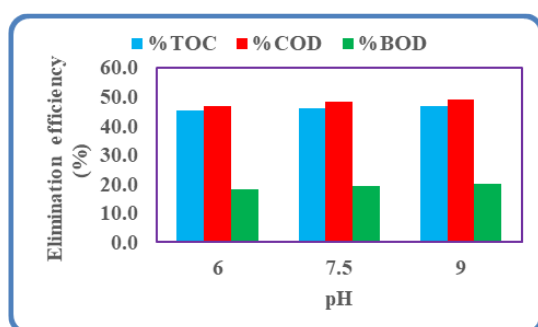


Fig. 8: % elimination efficiency versus pH.

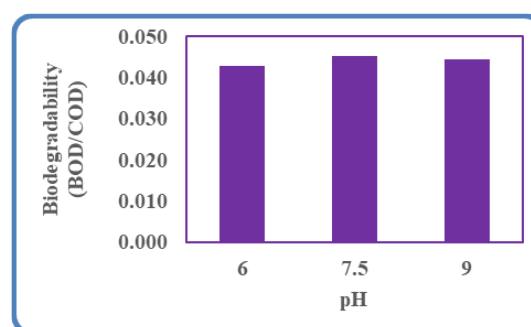


Fig. 9: Biodegradability (BOD/COD) versus pH.

3.4 RSM-Box Behnken Design Model Studies

In this method, Stat-Ease Inc.'s Design-Expert statistical software program, which is solely dedicated to doing the design of experiments (DOE), was used in the research. We

can perform comparative testing, screening, characterization, optimization, resilient parameter design, mixture designs, and integrated designs. A combination of three independent parameters T = pH, R = Dosage and S = Time, based on the Box Behnken Design model technique, was utilized. A quadratic polynomial surface methodology model statistical analysis was used according to Eq. 15 of BBD and a total of 15 experiments were found under the randomized subtype, as shown in Table 2.

$$N = 2 (K') (K' - 1) + (C_0) \tag{15}$$

where (K') = number of independent variables such as combined dosage, reaction time, and pH and Co = number of center points.

The highest and lowest variable's coded values were assigned as positive 1 and negative 1, as indicated in Table 3. These coded equations are extremely useful for identifying response factors by comparing factor coefficients.

Table 2: Experimental factors RSM-BBD method

Ver	11.1.1.0		
Type of Study	RSM-BBD	Subtype	Randomized type
Type of Design	Box-Behnken Design	Exp. Runs	15
Model	Quadratic polynomial	Blocks	No Blocks
Time (mins)	4.00		

Table 3: Independent variables employed

Factors	Independent Variable	Units	Type	Min.	Max.	Coded Low	Coded High	Mean	Std. Dev.
R	T : pH		Numeric	6	9	-1 ↔ 6	+1 ↔ 9	7.5	1.13
S	R : Dosage	(g/L)	Numeric	1	4	-1 ↔ 1	+1 ↔ 4	2.5	1.13
T	S : Time	(Minutes)	Numeric	60	300	-1 ↔ 60	+1 ↔ 300	180	90.71

The findings of the analysis of variance (ANOVA) for all the model responses, such as TOC, COD, BOD and biodegradability, are presented in Table 4-7. Using the ANOVA together with additional data like F-value, acceptable precision, coefficient of variance, probability value (Prob>F), and lack of fit, the model's validity and statistical significance (p<0.05) were assessed. The F-values of dependent variables TOC, COD, BOD and BOD/COD calculated were 14.2, 30.0, 43.3 and obtained P-values were 0.0047, 0.0001, 0.0003, respectively. The F-value and Prob>F values for the models and their independent parameters were significant because their p-values were less than 0.05, as indicated in Tables 4-7. Additionally, there was a 0.01 percent probability that noise could cause such a high F-value. Because they are not necessary to maintain the model hierarchy, model terms with p-values > 0.05 (not significant) were not taken into account via model reduction to improve the models [22]. The mathematical statistic model's coefficient of determination R² predicted R², adjusted R², and determined R² values for the desired responses of TOC, COD, BOD, and biodegradability were found to be 0.9623, 0.995, 0.9818 and 0.9873, respectively. According to adequate precision, the required responses were determined to be 12.80, 37.91, 17.86 and 19.95, all of which are more than 4. These values are utilized to calculate the signal-to-noise ratio and indicate that the empirical model has an appropriate signal and may be used to explore the design space. The R² value is more than 0.977, which is close to 1,

indicating that the model fits the data well and shows a strong correlation between the experimental and anticipated values [25].

Table 4: Analysis of Variance results for TOC elimination

Source	Sum of Squares	Degree of freedom	Avg. Square	F-value	P-value	
Design Model	3725.83	9	413.98	14.18	0.0047	significant
R: Dosage	2086.23	1	2086.23	71.44	0.0004	
S: Time	823.43	1	823.43	28.20	0.0032	
T: pH	54.19	1	54.19	1.86	0.2313	
RS	30.30	1	30.30	1.04	0.3551	
RT	0.0012	1	0.0012	0.0000	0.9951	
ST	0.0942	1	0.0942	0.0032	0.9569	
R ²	3.81	1	3.81	0.1305	0.7327	
S ²	661.21	1	661.21	22.64	0.0051	
T ²	82.13	1	82.13	2.81	0.1544	
Residual	146.01	5	29.20			
Lack of Fit	137.34	3	45.78	10.56	0.0877	not significant
Pure Error	8.67	2	4.33			
Cor Total	3871.84	14				

Table 5: Analysis of Variance results for COD elimination

Source	Sum of Squares	Degree of freedom	Avg. Square	F-value	P-value	
Design Model	3813.46	9	423.72	121.92	< 0.0001	significant
R: Dosage	2314.12	1	2314.12	665.88	< 0.0001	
S: Time	0.0189	1	0.0189	0.0054	0.9441	
T: pH	42.76	1	42.76	12.31	0.0171	
RS	68.14	1	68.14	19.61	0.0068	
RT	0.6833	1	0.6833	0.1966	0.6760	
ST	1.16	1	1.16	0.3346	0.5880	
R ²	180.73	1	180.73	52.01	0.0008	
S ²	1267.51	1	1267.51	364.72	< 0.0001	
T ²	2.46	1	2.46	0.7078	0.4385	
Residual	17.38	5	3.48			
Lack of Fit	16.71	3	5.57	16.71	0.0570	not significant
Pure Error	0.6667	2	0.3333			
Cor Total	3830.84	14				

Table 6: Analysis of Variance results for BOD elimination

Source	Sum of Squares	Degree of freedom	Avg. Square	F-value	P-value	
Design Model	295.92	9	32.88	29.95	0.0008	significant
R: Dosage	28.42	1	28.42	25.89	0.0038	
S: Time	84.98	1	84.98	77.42	0.0003	
T: pH	25.63	1	25.63	23.35	0.0047	
RS	1.02	1	1.02	0.9277	0.3797	
RT	0.2868	1	0.2868	0.2613	0.6310	
ST	0.0001	1	0.0001	0.0001	0.9928	
R ²	2.56	1	2.56	2.33	0.1876	
S ²	154.89	1	154.89	141.11	< 0.0001	
T ²	0.2232	1	0.2232	0.2034	0.6709	
Residual	5.49	5	1.10			not significant
Lack of Fit	4.82	3	1.61	4.82	0.1766	
Pure Error	0.6667	2	0.3333			
Cor Total	301.41	14				

Table 7: Analysis of Variance results for biodegradability

Source	Sum of Squares	Degree of freedom	Avg. Square	F-value	P-value	
Design Model	0.0021	9	0.0002	43.28	0.0003	significant
R: Dosage	0.0018	1	0.0018	338.13	< 0.0001	
S: Time	3.510E-07	1	3.510E-07	0.0656	0.8081	
T: pH	0.0000	1	0.0000	2.81	0.1542	
RS	8.959E-07	1	8.959E-07	0.1674	0.6994	
RT	6.455E-06	1	6.455E-06	1.21	0.3222	
ST	6.172E-08	1	6.172E-08	0.0115	0.9187	
R ²	0.0000	1	0.0000	2.86	0.1517	
S ²	0.0002	1	0.0002	40.62	0.0014	
T ²	0.0000	1	0.0000	7.95	0.0371	
Residual	0.0000	5	5.352E-06			not significant
Lack of Fit	0.0000	3	3.364E-06	0.4037	0.7684	
Pure Error	0.0000	2	8.333E-06			
Cor Total	0.0021	14				

To accommodate the experimental findings from the design runs carried out in connection with the configured Box Behnken Design, the response surface technique designs were either adopted or modified. Table 8 shows the responses of percentage elimination efficiencies of dependent variables. The RSM-BBD coded and actual components in terms of model equations were quadratic models [27], where R stands for dosage, S for reaction time, and T for pH level. The other terms, such as RS, RT, and TS, are the interaction terms. The square terms of dosage, reaction time, and pH were designated by R², S², and T² respectively. These equations can be used to anticipate responses for a given amount of each component, and coded factor equations help to determine the relative

effect factors by comparing factor coefficients. The actual coded equations, however, cannot be used for determination since the coefficients are scaled to accommodate the units of each factor rather than being at the center of the design space [28].

Table 8: Coded and Actual equations for all the responses

	Equations with coded factors	Equations with actual factors
TOC elimination (%)	$= + 40.33 + 16.15 (R) + 10.15 (S) + 2.60 (T) - 2.75 (RS) + 0.0173 (RT) - 0.1534 (ST) + 1.02 (R^2) - 13.38 (S^2) - 4.72 (T^2)$.	$= - 167.89300 + 11.20248 (R) + 0.463710 (S) + 33.31105 (T) - 0.015289 (RS) + 0.007694 (RT) - 0.000852 (ST) + 0.451526 (R^2) - 0.000929 (S^2) - 2.09612 (T^2)$
COD elimination (%)	$= + 62.33 + 17.01 (R) - 0.0486 (S) + 2.31 (T) - 4.13 (RS) - 0.4133 (RT) - 0.5392 (ST) - 7.00 (R^2) - 18.53 (S^2) - 0.8162 (T^2)$	$= - 76.83403 + 32.39084 (R) + 0.542583 (S) + 7.98120 (T) - 0.022929 (RS) - 0.183687 (RT) - 0.002996 (ST) - 3.10948 (R^2) - 0.001287 (S^2) - 0.362761 (T^2)$
BOD elimination (%)	$= + 21.33 + 1.88 (R) + 3.26 (S) + 1.79 (T) - 0.5045 (RS) - 0.2678 (RT) - 0.0050 (ST) - 0.8320 (R^2) - 6.48 (S^2) - 0.2459 (T^2)$	$= - 22.13268 + 4.50268 (R) + 0.195879 (S) + 3.12508 (T) - 0.002803 (RS) - 0.119007 (RT) + 0.000028 (ST) - 0.369756 (R^2) - 0.000450 (S^2) - 0.109285 (T^2)$
BOD/COD	$= + 0.0417 + 0.0150 (R) + 0.0002 (S) + 0.0014 (T) - 0.0005 (RS) + 0.0013 (RT) - 0.0001 (ST) - 0.0020 (R^2) - 0.0077 (S^2) - 0.0034 (T^2)$	$= - 0.089911 + 0.010788 (R) + 0.000205 (S) + 0.022264 (T) - 2.62921E-06 (RS) + 0.000565 (RT) - 6.90090E-07 (ST) - 0.000905 (R^2) - 0.5.32887E-07 (S^2) - 0.001509 (T^2)$

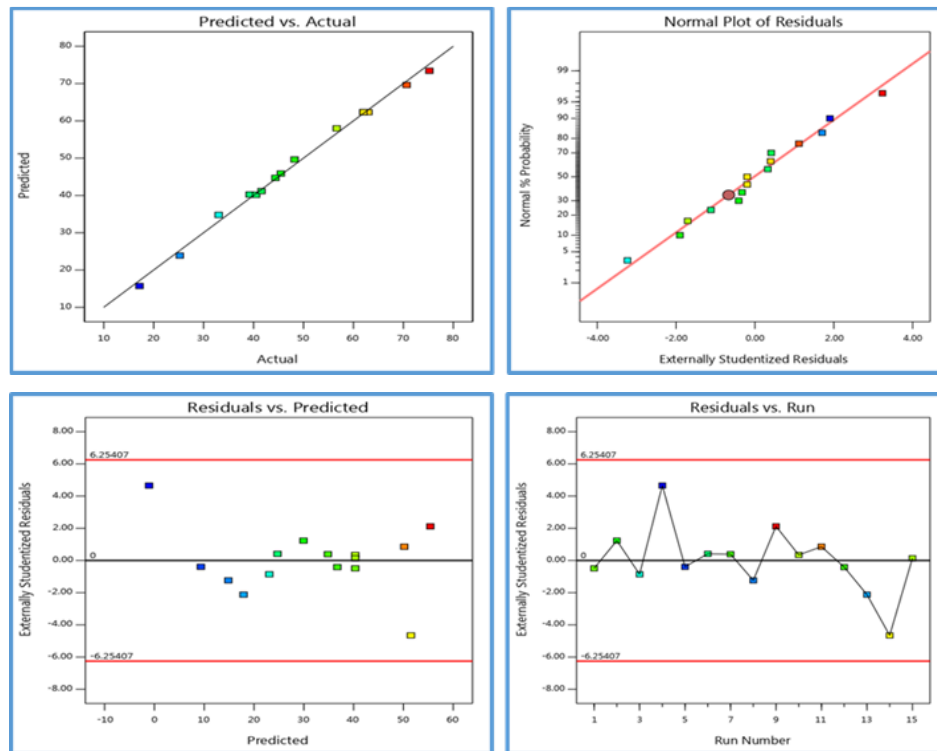
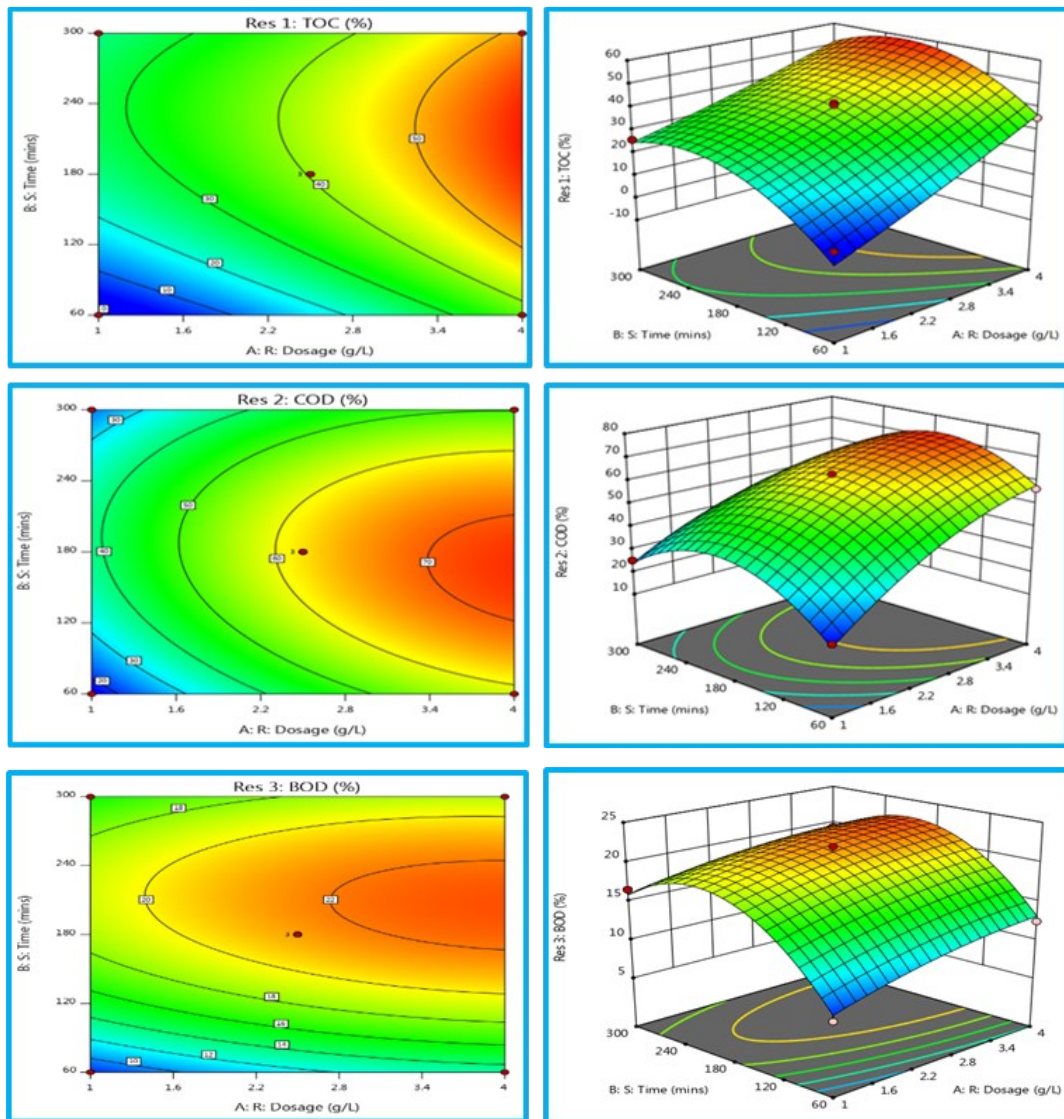


Fig. 10: RSM-BBD Predicted vs Actual and Normal plot of Residuals.

The plot of the predicted response against the internally studentized residuals in Fig. 10 provides graphic confirmation of the continuous variance assumption. The internally studentized residual values were obtained by dividing the residual values by the appropriate standard deviation. The sample points were dispersed randomly between the negative 6.25407 and positive 6.25407 outlier detection limits. Additionally, there were only slight differences between the actual and expected responses, indicating reasonable agreement between the predicted model and observed values. The described prediction model equations are thus considered adequate [29].

3.5 Interaction of 2-D Contour Plots and 3-D Surface Plots

Figure 11 depicts the cross-factor interaction effects between the independent predictors for eliminating dependent variables in photocatalytic seawater treatment using a combination using three-dimensional (3-D) surfaces and two-dimensional (2-D) contour plots. The maximum percentage elimination efficiencies as per RSM-BBD such as TOC = 55.4%, COD = 73.4%, BOD = 23.7%, and BOD/COD = 0.054 with a maximum effect of combined photocatalyst as 4 g/L, reaction time = 180 minutes and pH = 9.



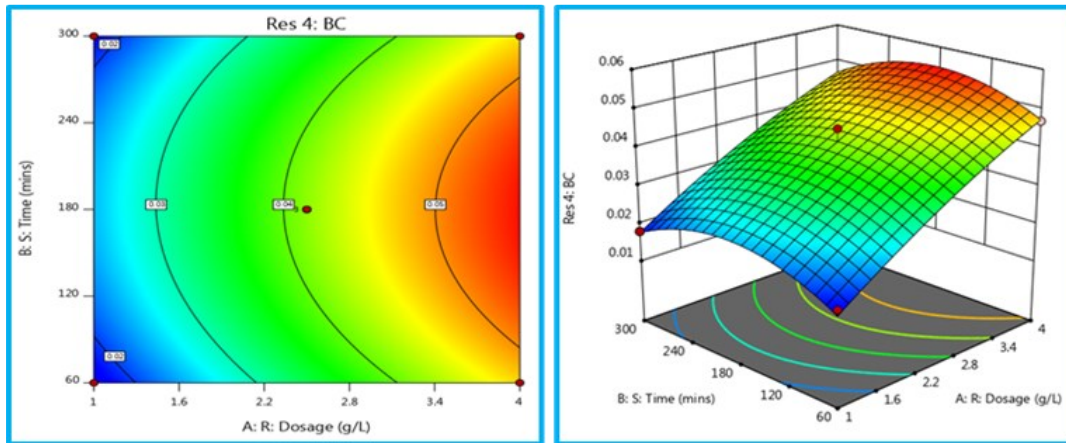


Fig. 11: 3D surface plots for all the responses.

3.6 Numerical Optimization of Model

The TiO_2 and ZnO combined photocatalyst load was set to 1, 2.5 and 4 g/L, the reaction duration was set to 60, 180 and 300 minutes and pH was set to 6, 7.5 and 9. These parameters were used in the RSM-BBD Design Expert software numerical optimization to maximize pollutant abatement. In addition, the output variables were set to optimum with a 95% confidence level. The desirability function approach was used, and the optimum circumstances obtained are depicted in the ramp function [32]. It is a function that uses a mathematical transformation to convert a multiple-response problem to a single-response problem. Finally, these function programs look for the option with the highest overall desirability. According to Fig. 12, the ramp function graph shows the desirability function of 0.972, 1 out of 36 solutions which are close to 1. The selected maximum values for the output variables of TOC = 58.1%, COD = 72.6%, BOD = 23.3% and biodegradability = 0.055, respectively, with an effect of combined catalyst as 4 g/L, pH = 8.266 and reaction time = 190.4 minutes.

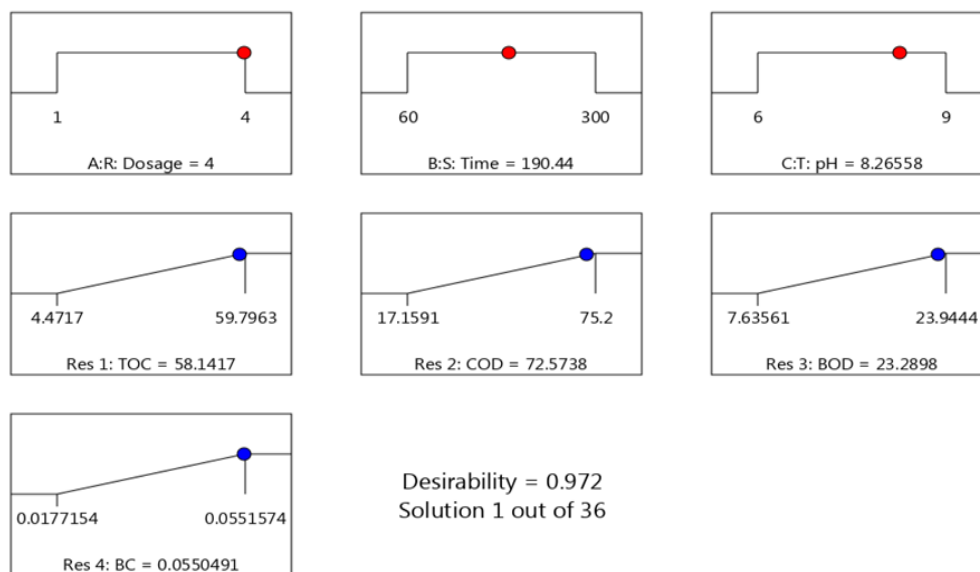


Fig. 12: RAMP function shows the desirability of the selected solution.

4. MATLAB ANFIS Based Statistical Modelling and Analysis

This section utilized the adaptive neuro-fuzzy inference system to optimize the responses. The first stage of this model is to initialize and optimize the (FIS) fuzzy inference system to represent the experimental data precisely, which can be accomplished by many procedures such as loading the experimental data sets, developing the FIS, training, and testing the (FIS) model. The ANFIS architectural network structure is depicted in Fig. 13.

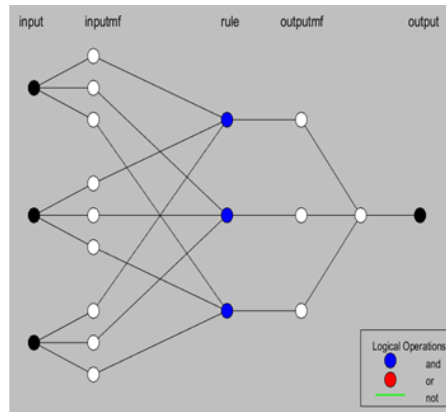


Fig. 13: Output network architecture for ANFIS model.

This ANFIS training approach incorporates the gradient descent and least square method. In this method, around 25% of the dataset was designated for testing, while 75% was used for training [35]. High correlation coefficients were used in its development for training, testing, and validation. The ANFIS model was developed with a high degree of correlation coefficient (i.e., 0.990) for the training, testing, and validation between the values. Using various membership functions for various combinations of the variables, the higher the R^2 ANFIS model was filtered. The models' effectiveness was assessed for both training and testing.

Table 9 displays the best clustering results, coefficient of determination (R^2), and root mean square error (RMSE). Figure 14 represents the RMSE analysis of training, testing, and overall datasets. It can be observed that RMSE for TOC and BOD are significantly less in comparison to COD data. However, the TOC and BOD's maximum value in the experiment set is 2.7 and 1.7. In contrast, COD ranges between 27 mg/L to 95 mg/L, and a deviation of 1.82 is minimal in corresponds to large values of COD. Figure 15 shows a correlation between the predicted and actual value in terms of R^2 value. Sample points closure to diagonal line gives a better R^2 value [37]. The simulation suggests that a small number of clustering in ANFIS modeling compared to a large number of clustering gives a better R^2 value.

Table 9: RMSE and R^2 values for the responses

Responses	No. of clusters	Training RMSE	Testing RMSE	All data RMSE	R^2 Analysis		
					Train data	Test data	All data
TOC	2	0.018	0.0374	0.023	0.998	0.999	0.998
BOD	2	0.009	0.017	0.010	0.992	0.988	0.991
COD	3	1.940	1.194	1.825	0.994	0.997	0.995

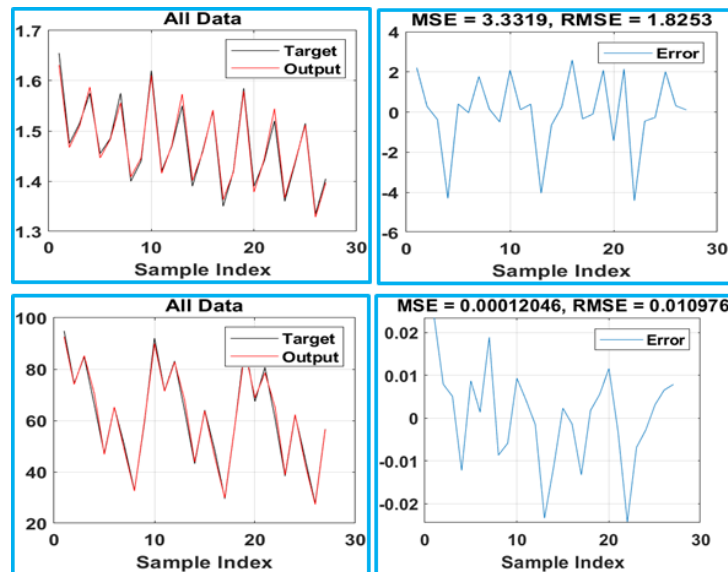


Fig. 14: Model predictions on training-testing data and its RMSE analysis.

The impact of Input parameters on a particular property can be analyzed by studying a 3D surface plot. Figure 16 shows the surface plots for three inputs, pH, dosage, and time. The experimental values or independent variables and the desired responses appeared to interact strongly, according to the surface plots [38]. Table 11 of the ANFIS statistical model shows that at a photocatalyst dose of 4 g/L, reaction time of 180 minutes and pH of 9, the maximum percentage elimination efficiency was found to be TOC=59.4%, COD=75.4%, BOD=24.2%, and biodegradability=0.055. Polynomial equation 16, using the mathematical formulation, is established to express the relationship between inputs and output [39]. Each polynomial equation correlates three inputs, i.e., dosage, time and pH, to one of the outputs, i.e., TOC, COD, BOD and BOD/COD. The polynomial equation is expressed below, where C is the coefficient, as listed in Table 10.

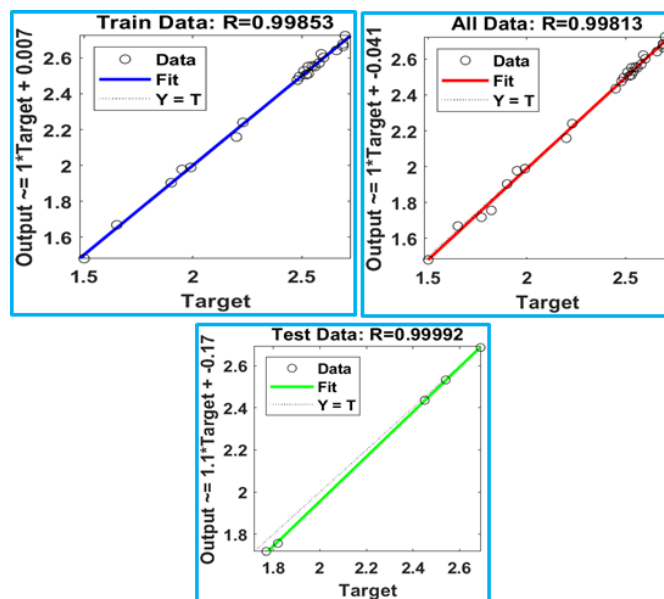


Fig. 15: Regression value for output responses.

$$O(D, t, P) = C_1D^3 + C_2D^2t + C_3D^2P + C_4D^2 + C_5Dt^2 + C_6DtP + C_7Dt + C_8DP^2 + C_9DP + C_{10}D + C_{11}t^2 - C_{12}t^2P + C_{13}t^2 + C_{14}tP^2 + C_{15}tP + C_{16}t + C_{17}P^3 + C_{18}P^2 + C_{19}P + C_{20} \quad (16)$$

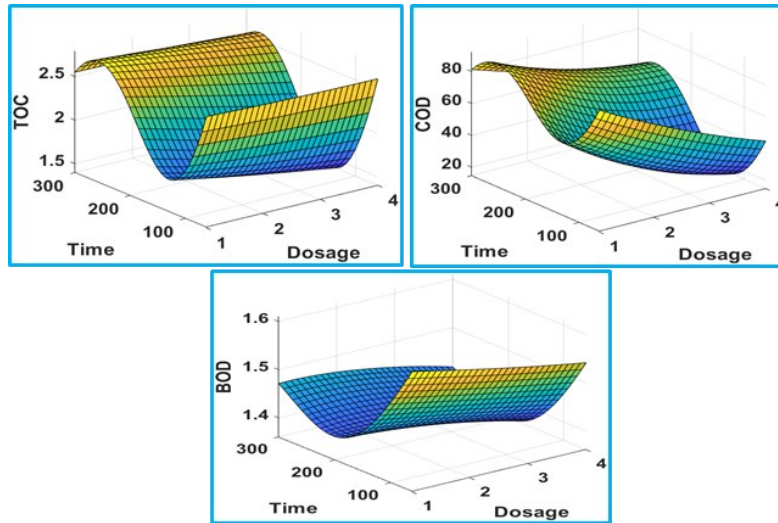


Fig. 16: 3D graph of regression for the responses.

Table 10: Coefficient value of polynomial equation expressed in the equation

Coefficient	TOC	COD	BOD
C1	-6.09154E+12	-3.54E+13	3.92837E+11
C2	0.000398538	7.92E-04	-7.58767E-05
C3	0.009997724	0.2850	0.001698481
C4	4.56866E+13	2.655E+14	-2.94628E+12
C5	9.31171E-06	0.000152428	5.78312E-08
C6	6.09955E-05	0.000706241	6.00877E-06
C7	-0.005512508	-0.038514773	0.000348171
C8	0.006051481	0.131168367	0.001380013
C9	-0.152814172	-3.4851686	-0.027966879
C10	-1.0051E+14	-5.84101E+14	6.48181E+12
C11	-682353.5565	-41651152.73	-1142667.33
C12	2.01832E-06	6.21677E-05	8.01073E-07
C13	368470920.5	22491622477	617040358.4
C14	6.72591E-05	0.000527089	1.9375E-07
C15	-0.001958112	-0.030065374	-0.000311682
C16	-56498874475	-3.44872E+12	-94612854956
C17	-3.65342E+11	9.39214E+11	68372164146
C18	8.22019E+12	-2.11323E+13	-1.53837E+12
C19	-6.08294E+13	1.56379E+14	1.1384E+13
C20	2.1109E+14	1.08568E+14	-2.79169E+13

5. CONCLUSION

The photocatalyst used in this study works well as a photocatalytic oxidizing agent for efficient seawater treatment. The experimental results showed that the optimum percentage elimination efficiency occurred at 4 g/L TiO₂ and ZnO doses, 180 minutes of reaction time

and pH 9. In addition, the biodegradability was found to be 0.055. The most significant removal efficiencies in terms of percentage were determined to be TOC=59.8, COD=75.2, BOD=23.9%, and biodegradability=0.055, respectively. According to RSM-BBD, the highest possible removal efficiencies were reported to be 55.4, 73.4, and 23.7% for TOC, COD, BOD and biodegradability as 0.054. Based on optimization criteria, a total of 36 solutions were discovered using RSM-BBD statistical modeling, and all of the response factors had a maximum desirability of 0.972 which is less than 1.0. The ANFIS was more precise with the prediction of TOC, COD, BOD, and biodegradability equal to 59.4, 75.4, 24.1, and 0.055, correspondingly with a dosage of 4 g/L, 180 mins reaction time and pH 9. ANFIS was also superior to RSM-BBD modeling's predictions, with an average R^2 value of 0.999 vs. 0.977. This research also indicated that the ANFIS model could be a helpful tool and a reliable alternative to the RSM-BBD model.

REFERENCES

- [1] Feroz S, Siyabi F, Dumaran JJC. (2014) Application of solar nano photo catalysis in treatment of seawater. *Int. Con. On Sust. Arch. and Environ. Eng.* 1:1-4.
- [2] Feroz S, Anna Jesil C. (2012) Treatment of organic pollutants by heterogeneous photo catalysis. *J. of the Inst. of Eng. (India): Ser. E*, 1: 45-48. <https://doi.org/10.1007/s40034-012-0001-6>
- [3] Jabri HA, Feroz S. (2015) Effect of combining TiO_2 and ZnO in the pretreatment of seawater reverse osmosis process. *Inter. J. of Environ. Sci. and Dev.* 6(5): 348-351.
- [4] Feroz S, Bawain M.S, Saadi S, Joy VM. (2015) Experimental studies for treatment of seawater in a recirculation batch reactor using TiO_2 P25 and polyamide. *Inter. J. of app. Eng. Res.*, 10: 26259-26266.
- [5] Feroz S, Raut NB, Maimani R. (2011) Utilization of solar energy in degrading organic pollutant – A case study. *Inter. J. of COMADEM.* 14(3): 33-37.
- [6] Xu H, Hao Z, Feng W, Wang T, Li Y. (2021) Mechanism of photo degradation of organic pollutants in seawater by TiO_2 – based photo catalysts and improvement in their performance, *American Chem. Soc.*, 6(45): 30698-30707. <https://doi.org/10.1021/acsomega.1c04604>
- [7] Azevedo EB, Torres AR, Neto FRA, Dezotti M. (2009) TiO_2 – photo catalyzed degradation of phenol in saline media in an annular reactor: hydrodynamics, lumped kinetics, intermediates and acute toxicity, *Brazilian J. Chem. Engr.*, 26(1): 75-87. <https://doi.org/10.1590/S0104-66322009000100008>
- [8] Qiuyi J, Xiaocai Y, Jian Z, Xinyang Q. (2017) Photocatalytic degradation of diesel pollutants in seawater by using ZrO_2 (Er^{3+})/ TiO_2 under visible light. *J. Environ. Chem. Engr.*, 5(2): 1423-1428. <https://doi.org/10.1016/j.jece.2017.01.011>
- [9] Al Deen D, Aljuboury A, Feroz S. (2021) Assessment of $TiO_2/ZnO/H_2O_2$ Photo catalyst to treat wastewater from oil refinery within visible light circumstances. *South African J. of Chem. Eng.* 35: 69-77. <https://doi.org/10.1016/j.sajce.2020.11.004>
- [10] Nayeemuddin M, Puganeshwary P, Feroz S. (2021) Pollutants removal from saline water by solar photo catalysis: a review of experimental and theoretical approaches. *Inter. J. of Environ. Anal. Chem.* 1-21. <https://doi.org/10.1080/03067319.2021.1924160>
- [11] Mashari MA, Varghese MJ, Feroz S, Rao LN. (2016) Characterization and photocatalytic treatment of oil produced water-using TiO_2 . *Int. J. of Apl of nanotechnology*, 3(1): 1-10.
- [12] Araimi M, Sangeetha BM, Feroz S, Saadi S. (2016) Treatment of seawater using solar energy in a recirculation pipe reactor. *Inter. J. for Inn. Res. in Sci & Tech.* 2(12): 2349-6010.
- [13] Jabri H, Hudaifi A, Feroz S, Marikar F, Baawain M. (2015) Investigation on the effect of TiO_2 and H_2O_2 for the treatment of inorganic carbon present in seawater, *Int. J. of Eng and Sci.* 5: 50-55.

- [14] Wang Z, Jia Y, Liu X, Liao L, Wang Z, Zheng. (2022) Removal of boron in desalinated seawater by magnetic metal-organic frame-based composite materials: Modeling and optimizing based on methodologies of response surface and artificial neural network. *J. of Mol. Liqs*, 349: 118090. <https://doi.org/10.1016/j.molliq.2021.118090>
- [15] Hashemi SH, Kaykhani M, Keikha AJ, Sajjadi Z. (2018) Application of Box-Behnken design in response surface methodology for the molecularly imprinted polymer pipette-tip solid phase extraction of methyl red from seawater samples and its determination by spectrophotometry. *Mar. Pol. Bul.* 137: 306-314. <https://doi.org/10.1016/j.marpolbul.2018.10.037>
- [16] Xu H, Hao Z, Feng W, Wang T, Fu X. (2022) The floating photo catalytic spheres loaded with weak light-driven TiO₂ –based catalysts for photodegrading tetracycline in seawater, 144: 106610. <https://doi.org/10.1016/j.mssp.2022.106610>
- [17] Kahani M, kalantary F, Soudi M.R, Pakdel L, Aghalizadeh S. (2020) Optimization of cost effective culture medium for *sporosarcina pasteurii* as biocementing agent using response surface methodology: Up cycling dairy waste and seawater. *J. of Clean. Prod.* 253: 120022. <https://doi.org/10.1016/j.jclepro.2020.120022>
- [18] Altayb HN, Kouidhi B, Baothman AS, Abdulhakim AJ, Ayed L, Hager M, Chaieb K. (2021) Mathematical modeling and optimization by the application of full factorial design and response surface methodology approach for decolourization of dyes by a newly isolated *Photo bacterium ganghwense*. *J. of Wat. Proc. Eng.* 44: 102429 <https://doi.org/10.1016/j.jwpe.2021.102429>
- [19] Vatanpour V, Sheydaei M, Esmaeili M. (2017) Box-Behnken design as a systematic approach to inspect correlation between synthesis conditions and desalination performance of TFC RO membranes. *Desal.* 420: 1-11. <https://doi.org/10.1016/j.desal.2017.06.022>
- [20] Peng X, Yang G, Shi Y, Zhou Y, Zhang M, Li S. (2020) Box-Behnken design based statistical modeling for the extraction and physicochemical properties of pectin from sunflower heads and the comparison with commercial low-methoxyl pectin. *Sci. Reports.* 10: 3595. <https://doi.org/10.1038/s41598-020-60339-1>
- [21] Mi H, Yi L, Wu Q, Xia J, Zhang B. (2021) Preparation and optimization of a low-cost adsorbent for heavy metal ions from red mud using fraction factorial design and Box-Behnken response methodology. *Cols. and Sur. A: Phy. and Eng. Asp.* 627:127198. <https://doi.org/10.1016/j.colsurfa.2021.127198>
- [22] Jaafarzadeh N, Zarghi MH, Salehin M, Roudbari A Zahedi A. (2020) Application of Box-Behnken Design (BBD) to optimizing COD removal from fresh leachate using combination of ultrasound and ultraviolet. *J. Environ. Treat. Tech.*, 8(3): 861-869.
- [23] Hout S, Salem Z, Tassalit D, Tigrine Z, Aburideh H. (2020) Assessing desalination pretreatment conditions towards pilot scale-up using Box-Behnken experimental design. *Wat. And Environ. J. Prom. Sus. sol.* 35(2): 473-485. <https://doi.org/10.1111/wej.12644>
- [24] Jamei M, Karbsi M, Malik A, Abualigah L, Islam ART, Yaseen ZM. (2022) Computational assessment of groundwater salinity distribution within coastal multi-aquifers of Bangladesh. *Sci. Rep.* 12:11165. <https://doi.org/10.1038/s41598-022-15104-x>
- [25] Boutra B, Sebti A, Trari M. (2022) Response surface methodology and artificial neural network for optimization and modeling the photo degradation of organic pollutants in water. *Inter. J. of Environ. Sci and Tech.* 19: 11263-11278. <https://doi.org/10.1007/s13762-021-03875-1>
- [26] Nayeemuddin M, Palaniandy P, Feroz S. (2022) Solar photocatalytic biodegradability of saline water: Optimization using RSM and ANN. *AIP Conf. Proc.* 2463, 1-11. <https://doi.org/10.1063/5.0080297>
- [27] Joy VM, Feroz S, Dutta S. (2020) TiO₂ / Photo-Fenton process for seawater pretreatment: modelling and optimization using response surface methodology (RSM) and artificial neural networks (ANN) coupled genetic algorithm (GA). *J. Indian Chem. Soc.*, 2:1:10. <https://doi.org/10.5281/zenodo.5657210>
- [28] Joy VM, Feroz S, Dutta S. (2021) Solar nano photocatalytic pretreatment of seawater: process optimization and performance evaluation using response surface methodology and genetic

- algorithm. *App. Water Sci.* 11:18. <https://doi.org/10.1007/s13201-020-01353-6>
- [29] Nayeemuddin M, Puganeshwary P, Feroz S. (2021) Optimization of solar photocatalytic biodegradability of seawater using statistical modelling. *J. the Indian Chem. Soc.* 98(12): 100240. <https://doi.org/10.1016/j.jics.2021.100240>
- [30] Miao T, Huang H, Guo J, Li G, Zhang Y, Chen N. (2022) Uncertainty analysis of numerical simulation of seawater intrusion using deep learning-based surrogate model. *Wat.* 14(18): 2933. <https://doi.org/10.3390/w14182933>
- [31] Kim CM, Parnichkun M. (2017) Prediction of settled water turbidity and optimal coagulant dosage in drinking water treatment plant using a hybrid model of k-means clustering and adaptive neuro-fuzzy inference system. *Appl. Water Sci.*, 7: 3885-3902. <https://doi.org/10.1007/s13201-017-0541-5>
- [32] Khayet M, Cojocar C, Essalhi M. (2011) Artificial neural network modelling and response surface methodology of desalination by reverse osmosis. *J. of Mem. Sci.* 368: 202-214. <https://doi.org/10.1016/j.memsci.2010.11.030>
- [33] Jia Y, Li J, Wang Z, Wu X, Xu K, Wang Z. (2020) Adsorption performance and response surface optimization of boron in desalinated seawater by UiO-66-NH₂. *Des. and Wat. Treat.* 197:157-169. <https://doi.org/10.5004/dwt.2020.25999>
- [34] Sibiya NP, Amo-Duodu G, Kweiyor Tetteh E, Rathilal S. (2022) Response surface optimization of a magnetic coagulation process for wastewater treatment via Box-Behnken. *Mat. Today: Proc.* 62: S122-S126, <https://doi.org/10.1016/j.matpr.2022.02.098>
- [35] Mahadeva R, Kumar M, Manik G, Patole SP. (2021) Modeling, simulation, and optimization of the membrane performance of seawater reverse osmosis desalination plant using neural network and fuzzy based soft computing techniques. *Des. and Wat. Treat.* 229:17-30. <https://doi.org/10.5004/dwt.2021.27386>
- [36] Ehteram M, Ahmed AN, Kumar P, Sherif M, Shafie AE. (2021) Predicting freshwater production and energy consumption in a seawater greenhouse based on ensemble frameworks using optimized multi-layer perceptron. *Energy Reports.* 7: 6308-6326. <https://doi.org/10.1016/j.egyrs.2021.09.079>
- [37] Najah A, El-Shafie A, Karim OA, El-Shafie AH. (2013) Performance of ANFIS versus MLP-NN dissolved oxygen prediction models in water quality monitoring. *Environ. Sci. Pollut. Res.* 21:1658-1670. <https://doi.org/10.1007/s11356-013-2048-4>
- [38] Jain A, Toussi IB, Mohammadian A, Bonakdari H, Sartaj M. (2022) Applications of ANFIS-type methods in simulation of systems in marine environments. *Math. Comput. Appl.* 27(29): 1-25. <https://doi.org/10.3390/mca27020029>
- [39] Mojarradi V, Sahraei S. (2020) Prediction of RO membrane performances by use of adaptive network-based fuzzy interference systems. *J. of Chem. and Petr. Eng.* 54(1): 99-110. <https://doi.org/10.22059/jchpe.2020.292454.1300>

Table 11. Shows the experimental, RSM and ANFIS values

Run	Input factors			TOC elimination (%)			COD elimination (%)			BOD removal (%)			BOD/COD		
	R : Dos (mg/L)	S : RT (min)	T : pH	Expt val.	BBD Pred. val.	Anfis Pred. val.	Expt val.	BBD Pred. val.	Anfis Pred. val.	Expt val.	BBD Pred. val.	Anfis Pred. val.	Expt val.	BBD Pred. val.	Anfis Pred. val.
1	2.5	180	7.5	38.000	40.330	39.580	62.000	62.330	62.310	21.000	21.330	21.300	0.040	0.042	0.039
2	2.5	300	6	33.104	29.930	33.519	41.589	41.170	41.264	15.677	16.070	15.143	0.030	0.030	0.028
3	1	180	9	20.692	23.070	22.900	39.223	40.240	37.962	20.771	20.430	20.520	0.021	0.021	0.020
4	1	60	7.5	4.472	4.300	4.519	17.159	15.720	18.929	7.636	8.380	7.917	0.018	0.016	0.018
5	2.5	60	6	8.178	9.330	7.900	40.523	40.190	36.404	10.589	9.570	8.345	0.029	0.029	0.025
6	1	300	7.5	25.938	24.720	24.348	25.232	23.880	25.428	16.583	15.900	15.562	0.018	0.018	0.018
7	2.5	300	9	35.986	34.830	38.310	44.377	44.710	43.840	18.642	19.660	18.610	0.032	0.032	0.023
8	2.5	60	9	11.673	12.850	12.240	45.468	45.890	41.253	13.534	13.140	11.869	0.031	0.032	0.024
9	4	180	9	59.796	55.400	59.386	75.200	73.430	75.392	23.944	23.660	24.138	0.055	0.054	0.055
10	2.5	180	7.5	42.000	40.330	35.580	62.000	62.330	60.496	21.000	21.330	20.864	0.040	0.042	0.032
11	4	180	6	52.539	50.160	53.740	70.646	69.630	70.672	20.275	20.620	18.948	0.049	0.049	0.044
12	4	60	7.5	35.501	36.720	35.454	56.641	57.990	58.731	12.475	13.150	12.297	0.047	0.047	0.034
13	1	180	6	13.504	17.900	15.005	33.015	34.790	33.271	16.031	16.310	15.390	0.020	0.021	0.020
14	4	300	7.5	45.959	51.510	45.282	48.205	49.640	47.776	19.405	18.660	18.191	0.045	0.047	0.025
15	2.5	180	7.5	41.000	40.330	38.580	63.000	62.330	61.900	22.000	21.330	20.864	0.045	0.042	0.032